Molecular Therapy
Methods & Clinical Development
Original Article

Gene editing-based targeted integration for correction of Wiskott-Aldrich syndrome

Melissa Pille,[1,8] John M. Avila,[2,8] So Hyun Park,[3,8] Cuong Q. Le,[2] Haipeng Xue,[2] Filomeen Haerynck,[4] Lavanya Saxena,[3] Ciaran Lee,[3,6] Elizabeth J. Shpall,[5] Gang Bao,[3] Bart Vandekerckhove,[1] and Brian R. Davis[2,7]

[1]Department of Diagnostic Sciences, Ghent University, 9000 Ghent, Belgium; [2]Brown Foundation Institute of Molecular Medicine, University of Texas Health Science Center at Houston, Houston, TX, USA; [3]Department of Bioengineering, Rice University, Houston, TX, USA; [4]Department of Internal Medicine and Pediatrics, Ghent University, 9000 Ghent, Belgium; [5]M.D. Anderson Cancer Center, Houston, TX, USA

Wiskott-Aldrich syndrome (WAS) is a severe X-linked primary immunodeficiency resulting from a diversity of mutations distributed across all 12 exons of the *WAS* gene. *WAS* encodes a hematopoietic-specific and developmentally regulated cytoplasmic protein (WASp). The objective of this study was to develop a gene correction strategy potentially applicable to most WAS patients by employing nuclease-mediated, site-specific integration of a corrective *WAS* gene sequence into the endogenous *WAS* chromosomal locus. In this study, we demonstrate the ability to target the integration of $WAS_{2\text{-}12}$-containing constructs into intron 1 of the endogenous *WAS* gene of primary $CD34^+$ hematopoietic stem and progenitor cells (HSPCs), as well as WASp-deficient B cell lines and WASp-deficient primary T cells. This intron 1 targeted integration (TI) approach proved to be quite efficient and restored WASp expression in treated cells. Furthermore, TI restored WASp-dependent function to WAS patient T cells. Edited $CD34^+$ HSPCs exhibited the capacity for multipotent differentiation to various hematopoietic lineages *in vitro* and in transplanted immunodeficient mice. This methodology offers a potential editing approach for treatment of WAS using patient's $CD34^+$ cells.

INTRODUCTION

Wiskott-Aldrich syndrome (WAS) is an X-linked primary immunodeficiency caused by mutations in the WAS gene, which encodes for the WAS protein (WASp). The WAS phenotype has been reported to be caused by a significant diversity of mutations distributed across the WAS genomic sequences.[1] WAS is characterized by recurrent infections, thrombocytopenia, eczema, severe immunodeficiency, and an increased risk of autoimmune diseases.[2–4] All hematopoietic cell lineages are affected in WAS. In addition to its role in phagocytosis and chemokine-induced migration, WASp is also known for its importance in T cell activation. WAS deficiency results in impaired immune synapse formation upon T cell activation which leads to ineffective proliferation and cytokine production upon CD3/CD28 activation.[5–8]

The first gene therapy for WAS, using gammaretroviral gene addition, showed significant restoration of WAS expression. WASp levels were restored in lymphoid and myeloid lineages and in platelets. Furthermore, the therapy restored the T cell function. Although the clinical status of the patients was improved, a high percentage of the patients developed acute leukemia due to insertional mutagenesis.[9] This prompted the development of lentiviral-based gene therapy. Lentiviral-mediated delivery of *WAS* cDNA to $CD34^+$ hematopoietic stem and progenitor cells (HSPCs) has shown sustained engraftment of the gene-modified cells with expression of WASp in lymphocytes and platelets.[10–14] All patients had improved immune function, fewer infections, and reduced bleeding. Very encouragingly, in a long-term follow-up study, vector integration site analysis showed no evidence for clonal expansion. However, complete restoration of the platelet deficit has proven challenging.

The objective of this study was to develop a gene editing-based methodology capable of treating the vast majority of WAS patients. The hypothesis was that targeted single-copy *WAS* transgene integration into the endogenous *WAS* locus will provide a more precise transgene integration as well as physiologically appropriate *WAS* transgene expression in HSPCs and HSPC-derived progeny. To obtain physiologic expression, the upstream promoter and regulatory sequences were fully preserved, and with the sole exception of transgene insertion into intron 1, the remainder of the WAS locus was left untouched. We recently demonstrated proof-of-principle for this targeted integration (TI) approach in WAS induced pluripotent stem cells (iPSCs).[15] Namely, we showed that homology-directed repair

Received 17 March 2023; accepted 2 February 2024;
https://doi.org/10.1016/j.omtm.2024.101208.

[6]Present address: School of Biochemistry and Cell Biology, University College Cork, Ireland

[7]Present address: University of Alabama at Birmingham, Birmingham, AL, USA

[8]These authors contributed equally

Correspondence: Gang Bao, Department of Bioengineering, Rice University, Houston, TX, USA.
E-mail: gb20@rice.edu
Correspondence: Bart Vandekerckhove, Department of Diagnostic Sciences, Ghent University, 9000 Ghent, Belgium.
E-mail: Bart.Vandekerckhove@UGent.be
Correspondence: Brian R. Davis, Brown Foundation Institute of Molecular Medicine, University of Texas Health Science Center at Houston, Houston, TX, USA.
E-mail: bdavis34@uab.edu

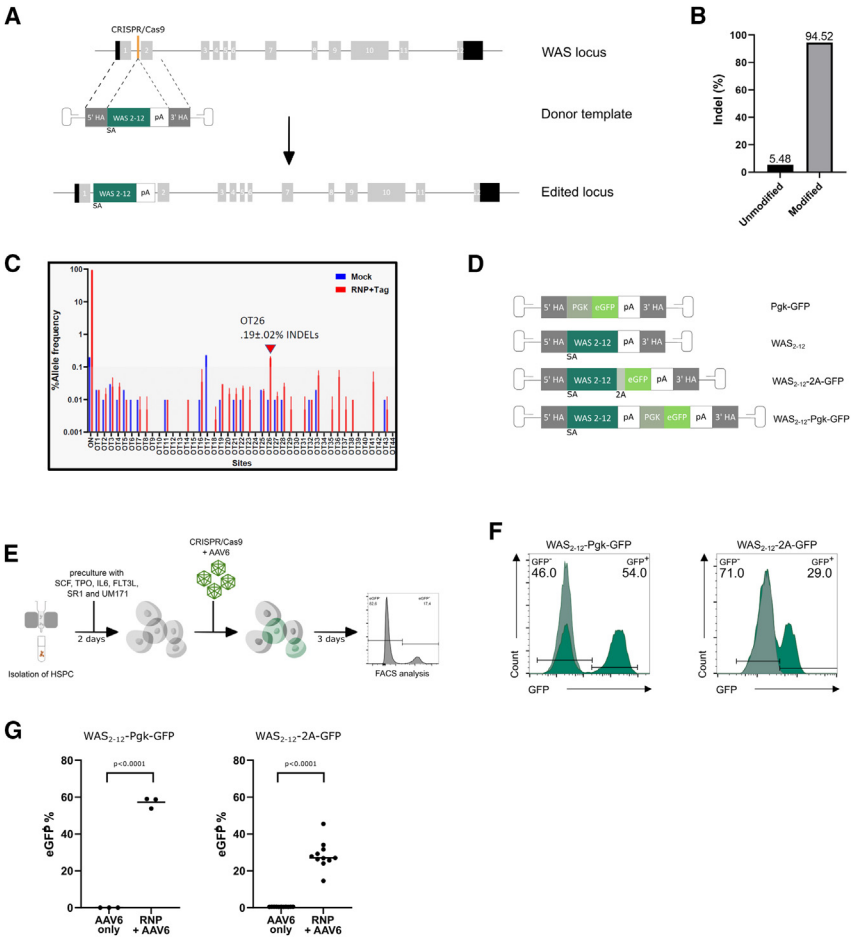

Figure 1. Targeted integration of *WAS$_{2-12}$* sequences into *WAS* intron 1 of normal male CD34$^+$ cells

(A) Schematic of *WAS* intron 1 targeted integration (TI) strategy. Shown is the location of CRISPR-Cas9 DNA cleavage in the endogenous *WAS* intron 1 (top diagram), the AAV6 delivered donor template (middle diagram), and the desired edited locus (bottom diagram).

(B) Percentage of *WAS* intron 1 sequences that were modified after electroporation of CD34$^+$ HSPCs with Cas9/gRNA RNP.

(C) Quantification of on-target (ON) and off-target (OT) activity by NGS and CRISPResso2 analysis of the ON and OT locations identified by COSMID (OT1-OT33) and GUIDE-seq (OT34-OT44).

(D) AAV-6 donor vectors employed in this study including therapeutic donors containing *WAS$_{2-12}$* cDNA, a splice acceptor (SA), poly(A) sequence (pA), 2A sequence (2A), phosphoglycerate kinase (PGK) promoter, and a GFP reporter gene (GFP).

(E) Experimental timeline for editing of primary CD34$^+$ HSPCs whereby these cells were isolated and pre-cultured for 2 days, electroporated with Cas9/gRNA RNP and subsequently transduced with AAV6 particles; and 3 days later, GFP positivity was determined through FACS analysis.

(F) FACS analysis of GFP expression in cord blood CD34$^+$ cells 3 days post editing using *WAS$_{2-12}$-Pgk-GFP* (left) or *WAS$_{2-12}$-2A-GFP* (right) donor vectors. The AAV6-only profile is shown in gray, with cells receiving both RNP and AAV6 vector shown in green.

(G) Frequency of GFP+ cells from experiments using primary CD34$^+$ cells treated with *WAS$_{2-12}$-Pgk-GFP* (AAV6-only or RNP+AAV6; n = 3 experiments with 2 technical replicates per experiment) or *WAS$_{2-12}$-2A-GFP* (n = 11 experiments with 2 technical replicates for 5 of the 11 experiments) donor vectors. HDR inferred by %GFP+ cells (n = 3 for *WAS$_{2-12}$-PGK-GFP* and n = 11 for *WAS$_{2-12}$-2A-GFP*, $p < 0.0001$, two-tailed unpaired t test). Data in Figure 1 are presented as mean ± SEM.

(HDR)-induced TI of a *WAS* exon 2–12 cDNA transgene (*WAS$_{2-12}$*) linked via 2A sequences to a GFP reporter (*WAS$_{2-12}$-2A-GFP*) into *WAS* intron 1 gave rise to appropriate hematopoietic-specific expression in progeny cells. All *WAS* mRNA in gene-corrected WAS iPSC-derived hematopoietic cells reflected splicing from the endogenous exon 1 to the corrective *WAS$_{2-12}$* transgene and not from splicing across the *WAS$_{2-12}$* transgene to endogenous mutant *WAS* genomic sequences.[15] Deficiencies in NK and T cell development and NK cell functions exhibited by WAS iPSC-derived cells were completely corrected by TI of the *WAS$_{2-12}$* cDNA. However, there are no robust protocols for generation of iPSC-derived HSPCs capable of long-term hematopoietic reconstitution. At present, a more tractable and translatable therapeutic approach would be to directly perform site-specific TI of the *WAS$_{2-12}$* transgene into intron 1 of the endogenous *WAS* locus of autologous CD34$^+$ HSPCs.

In this work, we developed a gene editing-based TI strategy targeting intron 1 of the WAS gene in CD34$^+$ HSPCs. We have demonstrated long-term engraftment and multipotent differentiation of edited CD34$^+$ HSPCs, and restored WASp expression in a WAS B cell line and WASp-dependent function in primary WAS T cells to levels comparable to healthy controls. These preclinical data support the feasibility of this therapeutic gene editing-based TI approach.

RESULTS

Targeted integration into intron 1 of the *WAS* locus

We previously targeted intron 1 of iPSCs of a WAS patient as shown in Figure 1A using zinc finger nucleases and a donor construct containing cDNA encoding *WAS* exons 2–12. Here, we used a similar strategy for gene editing CD34$^+$ HSPCs, except that we utilized CRISPR-guided Cas9 nucleases together with optimized gRNA sequences. Electroporation of normal (non-WAS) male CB CD34$^+$ cells with *WAS* intron 1 gRNA/Cas9 ribonucleoprotein complexes (RNPs) alone resulted in 94.5% of *WAS* intron 1 alleles exhibiting insertions/deletions (indels) as determined by next-generation sequencing (NGS) (Figure 1B. Off-target (OT) sites were identified using two methods (Figure 1C). Thirty-three potential OT sites (OT1-33) were identified *in silico* using COSMID[16] with settings allowing for

up to three mismatches or up to two mismatches plus a 1 bp indel. To further investigate the safety of our approach, 11 additional potential OT sites (OT34-44) were experimentally identified in $CD34^+$ cells via an unbiased, genome-wide analysis tool iGUIDE (genome wide, unbiased identification of double-strand breaks [DSBs] enabled by sequencing).[17,18] Subsequent NGS-based quantification of editing rates at these OT sites in RNP-treated $CD34^+$ cells indicate that no significant gene disruption occurred, since the indel frequencies were below the error rate of the illumina NGS platform (0.1%), except at OT26 (0.185% indel frequency). OT26 is located in an intronic region of a long noncoding RNA, which is 549 kb upstream and 74 kb downstream of known genes and is not known to be associated with disease, suggesting that this OT26 poses little safety issues for patients (Figure 1C, and Table S1). Next, donor templates were constructed encoding *Pgk-GFP*, $WAS_{2\text{-}12}$, or $WAS_{2\text{-}12}$*-2A-GFP* flanked by homology sequences to facilitate TI via HDR (Figure 1D).[15] As the *WAS* promoter may be too weak in primary $CD34^+$ HSPCs to obtain a strong GFP signal for the $WAS_{2\text{-}12}$*-2A-GFP* construct, a donor template with the strong *Pgk* promoter driving GFP expression was also generated ($WAS_{2\text{-}12}$*-Pgk-GFP)*. The experimental outline is shown in Figure 1E. $CD34^+$ HSPCs were expanded for 2 days before gene editing. AAV particles containing constructs with a GFP reporter were utilized to easily identify cells with TI. AAV-6 was selected for donor template delivery due to its tropism for human HSPCs as previously shown in $CD34^+$ cell gene editing.[19–21] TI efficiencies of 57.2% ± 2.9%, as measured by %GFP+ cells, were observed for the $WAS_{2\text{-}12}$*-Pgk-GFP* donor (Figures 1F and 1G). Similarly, the use of the $WAS_{2\text{-}12}$*-2A-GFP* donor resulted in TI efficiencies of 28.4% ± 7.5% (Figures 1F and 1G). Taken together, these data provide strong evidence for efficient $WAS_{2\text{-}12}$ TI.

On-target editing events mediated by $WAS_{2\text{-}12}$*-2A-GFP* and $WAS_{2\text{-}12}$*-Pgk-GFP* donors

To characterize gene editing outcomes at the endogenous *WAS* locus in greater detail, we first subjected an Epstein-Barr virus (EBV) transformed WAS B cell line (*WAS* mutation c.257G>A, Val75Met) to the aforementioned TI methodology utilizing the $WAS_{2\text{-}12}$*-2A-GFP* donor. After editing, the WAS B cells exhibited approximately 59.4% GFP+ cells (data not shown); cells were subsequently sorted for GFP+ (93.4% GFP+) and GFP− (99.9% GFP−) cells and further expanded in culture. We developed probe-based droplet digital PCR (ddPCR) copy number assays to quantify the rate of knockin (KI) at the on-target site by measuring the copy number of WAS alleles with KI at the left homology arm (LHA) or right homology arm (RHA) (Figures S1A and S1B). In male donors with one copy of the WAS allele, the percentage of the WAS allele with KI corresponds to the percentage of cells with KI. When the ddPCR assays were applied to the bulk edited (RNP+donor), GFP+ sorted, and GFP− sorted populations, they yielded percentages of KI at LHA/RHA of 49.2%/59.4%, 72.8%/83.2%, and 0.8%/1.6%, respectively (Figure 2A). In general, the LHA and RHA frequencies correlated roughly with the frequency of GFP+ cells as determined by fluorescence-activated cell sorting (FACS). However, we recognized that performing ddPCR at either end of the KI event would not capture the full spectrum of potential editing events.

Therefore, we combined long-range PCR together with single-molecule real-time sequencing (SMRT-seq) and unique molecular identifier (UMI) (Figure S2) to enable more accurate quantification of *WAS* alleles after editing.[22,23] The objective of the long-read sequencing methodology was to comprehensively catalog editing events, potentially including heterogeneous integration of the AAV donor or incomplete KI. When bulk edited cells were analyzed (Figures S3A and S3B), in addition to the expected events (unmodified [1,254 bp], small INDELs [1,180–1,304 bp], and the intended TI via the HDR pathway [3,740 bp]) (Figure S5A), we identified three other molecular species (Figures S3 and S4). The first was the consequence of a premature crossover event (Figure S5B) that caused a 61 bp deletion of intron 1 and integration only of the splice acceptor (1,193 bp). The premature crossover was promoted by the exact homology between *WAS* exon 2 sequences in the endogenous *WAS* locus and in the $WAS_{2\text{-}12}$ transgene donor. Thus, exon 2 of the transgene is used as an RHA resulting in the integration of the splice acceptor, but not the rest of the $WAS_{2\text{-}12}$*-2A-GFP* transgene due to the premature crossover. The second of these, occurring at very low frequency, consisted of asymmetric HDR alleles exhibiting HDR at the 5′ end together with NHEJ (non-homologous end-joining) induced KI at the 3′ end (4,293 bp) (Figure S5C); this resulted in two copies of the RHA with one copy of the AAV inverted terminal repeat between the two RHAs. Both HDR and 5′HDR + 3′NHEJ events were expected to result in the expression of the functional WAS and GFP under the endogenous *WAS* promoter. The third, again rare, were incomplete KI events (1,305 to 3,739 bp). The relative frequencies of these species are shown in Figure S3B. We note that the selection for GFP+ cells significantly enriched for the desired HDR-edited TI events (Figure S3B). Comparison of the FACS, ddPCR, and SMRT-seq results are shown in Figure 2A. For example, in RNP and $WAS_{2\text{-}12}$*-2A-GFP* donor-treated B cell line, we observed 59.4% GFP+ cells by flow cytometry, 49.2% KI at LHA by ddPCR, 59.4% KI at RHA by ddPCR and 45.6% HDR by SMRT-seq with UMI, which increased to 93.4%, 72.8%, 83.2%, and 98.7%, respectively, in GFP+ sorted cells (Figure 2A). Quantification of the donor integration rates using the three methods (FACS, ddPCR, and SMRT-seq with UMI) showed a good correlation. The relatively small discrepancies are likely due to the heterogeneous gene editing outcomes at *WAS* loci and the limitations of each quantification method.

We then proceeded to compare on-target integration in primary $CD34^+$ HSPCs for the $WAS_{2\text{-}12}$*-2A-GFP* and $WAS_{2\text{-}12}$*-Pgk-GFP* donors (Figure 2B). Based on the high frequency of premature crossover with the $WAS_{2\text{-}12}$*-2A-GFP* donor seen in the WAS B cell line, we added four silent mutations to exon 2 (and three silent mutations in exon 3) in the $WAS_{2\text{-}12}$*-Pgk-GFP* donor. Our rationale was to reduce the sequence similarity between the exon 2 sequences in $WAS_{2\text{-}12}$ and the endogenous exon 2 sequences in order to minimize premature crossover and maximize the desired targeted donor integration.[24] The frequency of GFP+ cells was measured by FACS, and

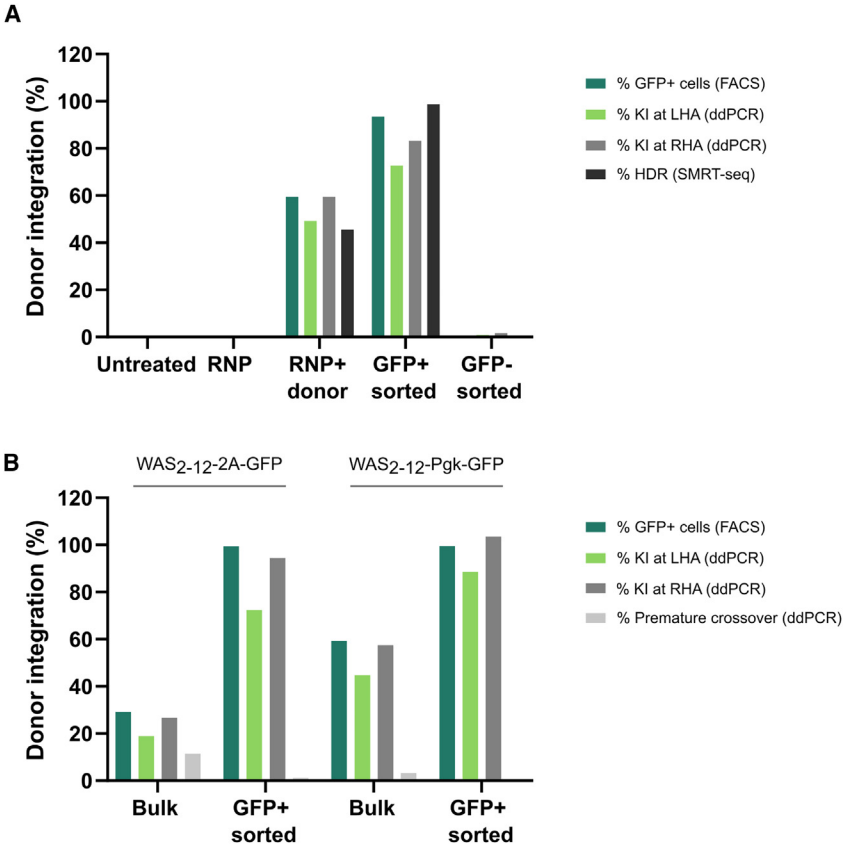

Figure 2. On-target editing events mediated by *WAS$_{2-12}$-2A-GFP* and *WAS$_{2-12}$-Pgk-GFP* donors

(A) On-target donor integration mediated by *WAS$_{2-12}$-2A-GFP* donor in WAS B cell line measured by FACS, ddPCR, and SMRT-seq with UMI. EBV-transformed WAS B cell line was edited with RNP only, and RNP along with *WAS$_{2-12}$-2A-GFP* donor and subsequently sorted for GFP+ and GFP− cells and further expanded in culture. On-target donor integration events in untreated, RNP-treated, RNP and donor-treated, GFP+ sorted and GFP− sorted cells were measured using three assays. The frequency of GFP+ cells was measured by FACS, frequencies of KI at LHA and RHA were quantified by probe-based ddPCR assays, and the frequency of HDR was quantified by SMRT-seq with UMI. The LHA and RHA KI frequencies and HDR frequencies correlated roughly with the frequency of GFP+ cells.

(B) On-target donor integration mediated by *WAS$_{2-12}$-2A-GFP* vs. *WAS$_{2-12}$-Pgk-GFP* donors measured by FACS and ddPCR. Primary CD34$^+$ HSPCs were edited with RNP along with *WAS$_{2-12}$-2A-GFP* or *WAS$_{2-12}$-Pgk-GFP* donors. In bulk edited (RNP+donor) samples, the use of the *WAS$_{2-12}$-Pgk-GFP* donor vs. *WAS$_{2-12}$-2A-GFP* donor resulted in an increased frequency of GFP+ cells. Evagreen-based ddPCR confirmed an increase in targeted donor integration for *WAS$_{2-12}$-Pgk-GFP* and a decrease in premature crossover compared with *WAS$_{2-12}$-2A-GFP* donor. Sorting for GFP+ cells yielded a population of cells almost completely devoid of cells with the premature crossover allele. The frequency of KI at RHA is consistent with the frequency of GFP+ cells.

the frequencies of KI at LHA and RHA and premature crossover were quantified by ddPCR. In bulk edited (RNP+donor) samples, the use of the *WAS$_{2-12}$-Pgk-GFP* donor vs. *WAS$_{2-12}$-2A-GFP* donor resulted in an increased frequency of GFP+ cells (59.2% vs. 29.1%); these results are consistent with that shown in Figures 1F and 1G ddPCR confirmed an increase in donor integration at LHA and RHA for *WAS$_{2-12}$-Pgk-GFP* vs. *WAS$_{2-12}$-2A-GFP* (LHA/RHA: 44.8%/57.4% vs. 18.9%/26.6%) and a decrease in premature crossover (3.3% vs. 11.4%). Thus, we chose to use the *WAS$_{2-12}$-Pgk-GFP* donor for subsequent experiments with CD34$^+$ HSPCs. Irrespective of the donor utilized, sorting for GFP+ cells yielded a population of cells almost completely devoid of cells with the premature crossover allele. Although there are inherent limitations to the molecular methods employed (see discussion), the quantification of sorted GFP+ cells using ddPCR and SMRT-seq together with UMI (Figure 2A and 2B) is consistent with all or nearly all GFP+ cells exhibiting *WAS* intron 1 TI.

TI of CD34$^+$ cells results in marking of all major hematopoietic lineages

Next, we aimed to demonstrate that TI-marked CD34$^+$ HSPCs, identified by and sorted for GFP expression, were capable of *in vitro* differentiation into various hematopoietic cell types similar to wild-type CD34$^+$ cells (Figure 3A). Cord blood-derived healthy CD34$^+$ HSPCs were edited utilizing the *WAS$_{2-12}$-Pgk-GFP* donor. GFP+ and GFP− cells were sorted 3 days later and subsequently cultured under various conditions optimized to generate erythroid, megakaryocytic, myeloid, NK and B cell hematopoietic lineages (Figure 3A). Cell cultures were supplemented once a week (erythrocytes and NK cells) or transferred to a new monolayer every week (B cells and myeloid cells or every other week [NK cells]). After 2–4 weeks, depending on the lineage of interest, cells were harvested and analyzed by flow cytometry. Both GFP+ TI and GFP− wild-type cells were differentiated to CD71$^+$CD235$^+$ erythrocytes and CD42$^+$CD41b$^+$ megakaryocytes to the same extent (Figures 3B and 3C) after 14 days of culture. Furthermore, no major differences were found in the generation of CD56$^+$CD94$^+$ NK cells after 4 weeks, nor in the generation of CD20$^+$CD19$^+$ B cells. Marked progeny cells also included CD14$^+$CD4$^+$ monocytes and CD15$^+$HLA-DR + granulocytes (Figures 3B and 3C). T cell precursor activity was not tested. Overall, these data suggest that TI occurred in progenitors that were able to differentiate into all major hematopoietic lineages. Besides the capacity of the corrected HSPC population to differentiate into all hematopoietic lineages, these HSPCs need to be able to engraft and repopulate immunodeficient NOD-*scid* IL2Rgamma^{null} (NSG) mice. For these experiments, we edited CD34$^+$ HSPCs isolated either from cord blood (HSPC-C) or from mobilized peripheral blood obtained by apheresis (HSPC-A) (Figure S6A). Cells were cultured overnight

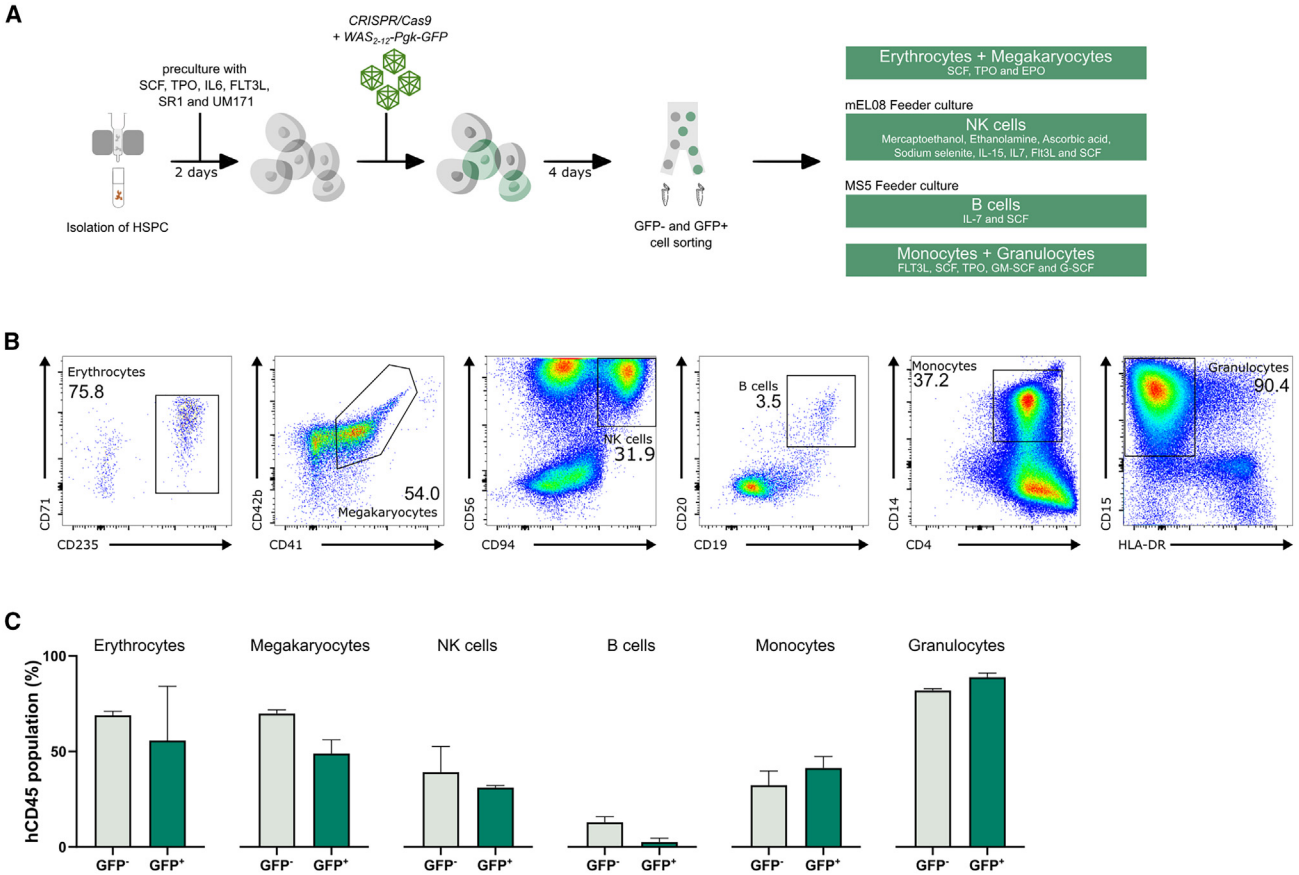

Figure 3. Multipotential *in vitro* hematopoietic differentiation of *WAS* TI normal CD34$^+$ cells

(A) Experimental timeline for editing and hematopoietic differentiation of primary CD34$^+$ cells.

(B) Differentiation toward the various hematopoietic cell lineages of GFP$^+$ edited CD34$^+$ cells: CD235$^+$CD71^{dim} erythrocytes, CD42b$^+$CD41$^+$ megakaryocytes, CD56$^+$CD94$^+$ NK cells, CD20$^+$CD19$^+$ B cells, CD14$^+$CD4$^+$ monocytes, CD15$^+$HLA-DR$^-$ granulocytes. Histograms show representative examples per population.

(C) Frequency of differentiated cell types generated from either GFP− or edited GFP+ CD34$^+$ cells. Data are presented as mean ± SEM (n = 2).

in cytokine rich medium at 5% O_2, as described by Bak et al..[21] Next, the HSPC-C and HSPC-A were electroporated with RNPs and AAV-6 *$WAS_{2\text{-}12}$-Pgk-GFP* donor transduced using our standard protocol. A total of 3 × 10^5 electroporated, transduced, non-sorted cells were injected intrahepatically into NSG pups (HSPC-C) or intravenously in the tail of adult NSG mice (HSPC-A) together with a control group injected with non-edited precursors. All mice survived the procedure. Thymus, spleen, and bone marrow were harvested 10 weeks later and analyzed by flow cytometry. Flow cytometric analysis of bone marrow showed that within the human CD45$^+$ population, edited CD34$^+$ HSPCs were still abundantly present 10 weeks after transplantation (Figures 4A and 4B). In addition, granulocytes, monocytes, T cells, B cells, and NK cells showed no significant difference in lineage distribution in the GFP+, GFP−, and mock populations. Furthermore, no significant differences were found in the cell-type distribution in the spleen of these mice where the B-lineage forms the majority of the populating cells (Figures 4C and 4D). Note here the presence of a small but distinct T cell population in both the GFP+ and GFP− populations, indicating that T cell precursors are gene edited. Similar results were obtained after the transplantation of adult HSPC-A in adult transplanted mice, a model more similar to clinical transplantation practice (Figures 4E–4H). Importantly, GFP+ CD34$^+$ HSPCs were still abundantly present in the bone marrow of HSPC-A transplanted mice. The presence of GFP+ lymphoid or myeloid cells in bone marrow and spleen demonstrates the ability of edited cells to give rise *in vivo* to a variety of differentiated cell types, consistent with the *in vitro* differentiation experiments. Furthermore, the presence of GFP+ CD34$^+$ cells in the bone marrow 10 weeks after transplantation is consistent with marking of hematopoietic progenitors that can support long-term blood cell production and/or with marking of repopulating HSPCs.

Restoration of WASp expression in TI-treated cells

We previously described (Figure 2A) performing TI with *$WAS_{2\text{-}12}$-2A-GFP* (Figure 5A) in an EBV transformed male WAS B cell line and subsequently sorting and expanding GFP+ cells. Here, we utilize the GFP+ sorted cells to demonstrate TI-mediated full restoration of WASp expression. To compare with lentivirus transduced cells, we

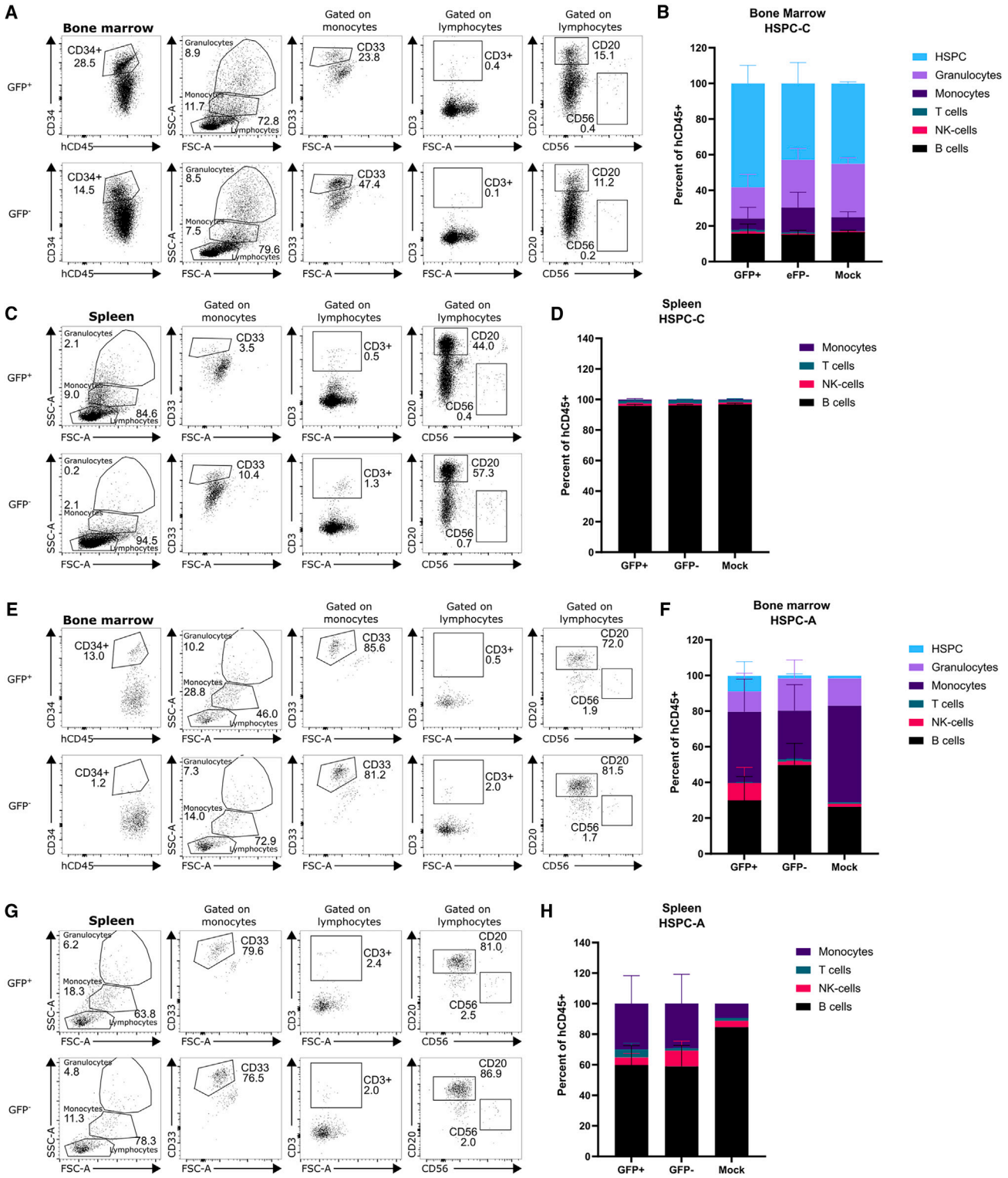

Figure 4. Multipotential *in vivo* hematopoietic differentiation of *WAS* TI normal CD34⁺ cells

(A) Flow cytometric dot plots showing HPSC, granulocytes, monocytes, mature T cells, B cells, and NK cells in bone marrow of animals injected with HSPC-C 10 weeks after transplantation.

(legend continued on next page)

generated the lentiviral construct pRRLSIN.cPPT.W1.6-$WAS_{1\text{-}12}$-2A-GFP.WPRE in which the *WAS* 1.6 kb promoter sequences ($W1.6_p$) directed expression of $WAS_{1\text{-}12}$-*2A-GFP* (Figure 5A). After production, purification, and titration of the VSV-G enveloped lentiviral vector, we identified transduction conditions for the aforementioned EBV-transformed WAS B cell line that favored generation and isolation of GFP+ single-cell-derived clones bearing a single copy lentiviral integrant per cell (materials and methods). Such a clonal GFP+ cell line was evaluated for restoration of WASp expression by western blot (Figure 5B). Due to residual 2A sequences (19 amino acids) at the COOH-terminal end of WASp, the transgenic WASp resulting either from TI or lentiviral transduction can be distinguished from wild-type WASp[15] due to the somewhat higher molecular weight (Figure 5B). TI cells exhibited restoration of WASp expression. Furthermore, in contrast to $W1.6_p$-$WAS_{1\text{-}12}$-*2A-GFP* lentivirus transduced cells, $WAS_{2\text{-}12}$-*2A-GFP* TI cells only expressed the corrected WASp, with the endogenous mutant WASp not being expressed (Figure 5B). This result (i.e., the absence of expression of the endogenous mutant WASp) is what would be expected from successful single copy TI per *WAS* allele in male cells provided there is efficient splicing from exon 1 to the $WAS_{2\text{-}12}$ transgene.

Functional restoration in TI-treated T cells

Restoration of WASp expression and WASp-dependent function was assessed in primary T cells from a WAS patient with a frameshift mutation in the *WAS* gene (c.361 365delGATCG). The experimental timeline is shown in Figure 6A. After pre-stimulation, WAS T cells underwent TI with the $WAS_{2\text{-}12}$-*Pgk-GFP* donor. Mean percentage of GFP+ cells was 9% (data not shown). GFP+ cells ("Corrected WAS Patient") and GFP− cells ("WAS Patient") were sorted and analyzed for expression of cytoplasmic WASp by FACS (Figures 6B and 6C). WASp expression levels in a positive control (healthy control T cells [WT]) and a negative control (Cas9/WAS exon 2-mediated WASp knockout in healthy control T cells ["$WAS^{k/o}$"]) (Figure 6C) were included. TI restored WASp expression to *WAS* mutant T cells at a level comparable to unmanipulated, normal T cells ("WT") (Figure 6C). Next, we studied the functional properties of TI T cells. GFP+ (corrected) vs. GFP− (uncorrected) T cells were subjected to overnight IL-2 starvation followed by αCD3/αCD28 stimulation and subsequently analyzed for evidence of restored WASp-dependent function. Importantly, corrected WAS patient T cells exhibited restored production of IL-2 and IFN-γ (Figure 6D). There was a 2-fold increase in the IFN-γ production and a 5-fold increase in IL-2 production in corrected cells. The corrected WAS patient T cells showed increased proliferation upon stimulation with αCD3/αCD28 for 6 days (Figure 6E). Furthermore, corrected T cells exhibited improved upregulation of the activation markers CD69 and CD137 upon stimulation with suboptimal CD3 concentrations. Also note the enhanced actin-mediated downmodulation of the CD3/TCR complex upon αCD3/αCD28 stimulation (Figure 6F). Finally, to demonstrate functional correction of actin filament formation, we visualized the immune synapse forming at the contact area with αCD3-coated beads by staining of the actin cytoskeleton. GFP+ and GFP− cells were incubated with Dynabeads in a 2:1 bead-to-cell ratio. Cells were then transferred to poly-L-lysine-coated plates, fixated and stained with phalloidin overnight. The next day, after DAPI staining, cells were analyzed under a confocal laser scanning microscope. The actin immune synapse did not form in uncorrected WAS T cells but was prominently present in corrected WAS T cells (Figure 6G). Taken together, we showed TI-mediated restoration of WASp-dependent T cell function using multiple assays.

DISCUSSION

In this study, we developed a gene editing-based TI strategy targeting intron 1 of the *WAS* gene in $CD34^+$ HSPCs. We have demonstrated engraftment and multipotent differentiation of edited $CD34^+$ HSPCs. This approach restored WASp expression in a WAS B cell line and primary WAS T cells to levels comparable to healthy controls. Furthermore, we showed that TI prevented the expression of the defective WASp. Finally, TI restored WASp-dependent function in primary WAS T cells. These data are consistent with our previous report of intron 1 $WAS_{2\text{-}12}$ TI correction of WAS iPSCs. These preclinical data support the feasibility of this therapeutic gene editing-based TI approach in man.

Our objective in targeting *WAS* intron 1 was to develop a methodology capable of correcting for a diversity of mutations spread across the WAS gene, while preserving appropriately regulated levels of WAS expression. With this approach, approximately 85% of WAS patients (those not carrying mutations in WAS exon 1) could potentially be treated.[25] The most severe WAS cases are generally those in which there is no expressed WASp and these are the main candidates for gene therapies such as gene delivery or gene editing. Targeted sequence-specific gene insertion in the endogenous *WAS* gene, in comparison with the lentiviral gene delivery approach, offers, in principle, the potential advantages of a more defined integration profile

(B) Lineage distribution within BM $hCD45^+$ cells in animals transplanted with HSPC-C (n = 6 mice for all groups except for mock, n = 3); no significant differences in lineage distribution were observed for GFP+ and GFP− populations.
(C) Flow cytometric dot plots showing the presence of granulocytes, monocytes, T cells, B cells, and NK cells in spleens of animals transplanted with HSPC-C.
(D) Lineage distribution within spleen $hCD45^+$ cells in animals injected with HPC-C (n = 6 mice for all groups except for mock, n = 3); no significant differences observed in lineage distribution.
(E) Flow cytometric dot plots showing the presence of HSPCs, granulocytes, monocytes, T cells, B cells, and NK cells in bone marrow of animals transplanted with HSPC-A.
(F) Lineage distribution within BM $hCD45^+$ cells of animals injected with HSPC-A (n = 4 mice for all groups except for mock, n = 1); no significant differences between groups in lineage distribution.
(G) Flow cytometric dot plots showing the presence of granulocytes, monocytes, T cells, B cells, and NK cells in spleens of animals transplanted with HPC-A.
(H) Lineage distribution within spleen $hCD45^+$ cells (n = 4 mice for all groups except for mock, n = 1) of animals injected with HSPC-A; no significant differences. Data are presented as mean ± SEM. p values were calculated using two-tailed unpaired t test (B) and two-way ANOVA with Tukey's multiple comparisons test (B–D and F–H).

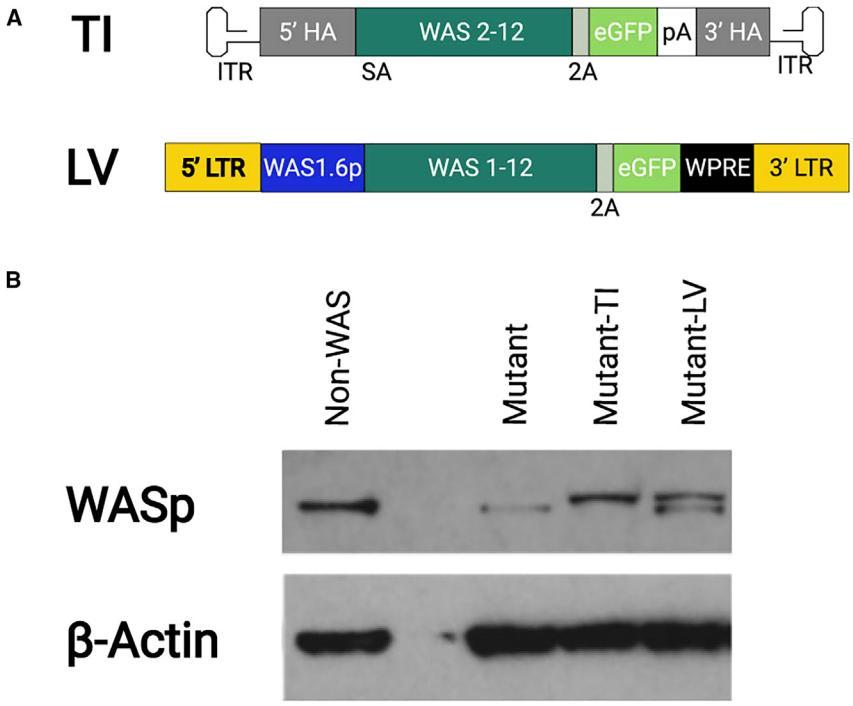

Figure 5. Comparison of TI and lentiviral approaches for restoration of WASp expression in a *WAS* mutant B lymphoblastic cell line

(A) Schematic of the AAV6 $WAS_{2\text{-}12}$-2A-GFP donor (TI) utilized in intron 1 TI of *WAS* mutant (*WAS* genotype) and the lentivirus (LV) construct used for transduction of the same cell line.

(B) Western blot analysis of WASp expression in WAS B cells, either unmodified ("Mutant"), subjected to TI and subsequently enriched for GFP-expressing cells ("Mutant-TI"; ∼65% GFP expressing), or transduced with LV and GFP sorted and expanded ("Mutant-LV"). Normal ("Non-WAS") served as a positive control. β-actin immunostaining as control for equal loading.

and regulated, cell-type-specific restoration of WASp expression directed by the endogenous *WAS* locus. On the other hand, a significant frequency of *WAS* mutations is missense or frameshift, with some of these mutations giving rise to mutant WASp still present in cells (e.g., as seen for the c.257G>A (Val75Met) WAS B cell line (Figure 5).[26] For such cases, the intron 1 TI strategy perhaps offers advantages compared with a lentivirus-based approach in which both the endogenous mutant WASp and exogenous WT WASp are co-expressed in transduced cells. We also note that some *WAS* mutations give rise to an expressed WASp that may function in a dominant negative manner (e.g., 1305delG)[27] and could therefore compete with the exogenous WT WASp when using the lentiviral approach.

Recent studies have revealed complex mis-integration profiles in CRISPR KI experiments at the Cas9 on-target cut-site, including incomplete integration, asymmetric HDR (defined as repair events showing a proper HDR junction at one of the two homology arms, while repair at the other homology arm resolves through a non-HDR mechanism), AAV capture and AAV concatemer capture.[28,29] Although primarily maintained in an episomal state, AAV genome can be integrated into the host genome at CRISPR on-target and OT cut-sites.[30] Currently no single tool can detect all the complex integration outcomes, especially events occurring with very low frequencies.[31] Therefore, we used three assays, FACS, ddPCR, and SMRT-seq with UMI, to comprehensively quantify the molecular events due to gene editing. FACS quantifies the percentage of cells with $WAS_{2\text{-}12}$-*Pgk-GFP* integrated into the genome at on-target and OT sites regardless of the type of integration event. However, for $WAS_{2\text{-}12}$-*2A-GFP*, due to the absence of a promoter, detection of OT integration is more difficult. Furthermore, HDR-mediated TI, the capture of AAV or AAV concatemers, or incomplete integration of truncated Pgk-GFP are expected to produce GFP+ cells. Probe-based ddPCR copy number assays were developed to quantify the rate of KI at the on-target site. However, we recognized that performing ddPCR at either end of the KI junction would not capture the full spectrum of potential editing events. In addition, ddPCR quantifies WAS alleles that generate amplicon across the KI junction without providing sequence information, making it difficult to identify which KI event leads to a positive ddPCR result. Therefore, we used long-range PCR and SMRT-seq with UMI (Figure S2) to enable more accurate quantification of *WAS* alleles after editing[22,23] However, we note that enrichment of long amplicons can only be used to examine large deletions and insertions of several kb due to technical limitations of long-range PCR. Large deletions that remove the primer binding site are undetectable and large insertions such as AAV concatemer integration can be missed or underestimated by SMRT-seq. Therefore, using the combination of three assays, FACS, ddPCR, and SMRT-seq with UMI, allowed us to detect a wider range of the molecular events than any of the tools alone. A catalog of the resultant molecular species, summarized in Figure S4, gives the details of the three species that were anticipated: unmodified, indels, and the intended HDR at both LHA and RHA. In addition, we observed premature crossover events when using either the $WAS_{2\text{-}12}$-*2A-GFP* or $WAS_{2\text{-}12}$-*Pgk-GFP* donor. Although occurring at significantly lower frequencies, we did observe events with HDR on one side and NHEJ on the other side of the cut-site and events reflecting an incomplete KI.

We first evaluated a donor in which $WAS_{2\text{-}12}$ sequences were linked to a GFP reporter via 2A sequences. This design was the same as employed in our prior correction of WAS iPSCs.[15] In this case, GFP reporter expression would be governed by the endogenous *WAS* promoter and regulatory sequences; in addition, the level of GFP expression would track that of the *WAS* transgene. Although we could clearly identify GFP expression following editing of primary $CD34^+$ cells, the relatively low level of endogenous WAS expression in HSPCs made this donor less than ideal for isolation of

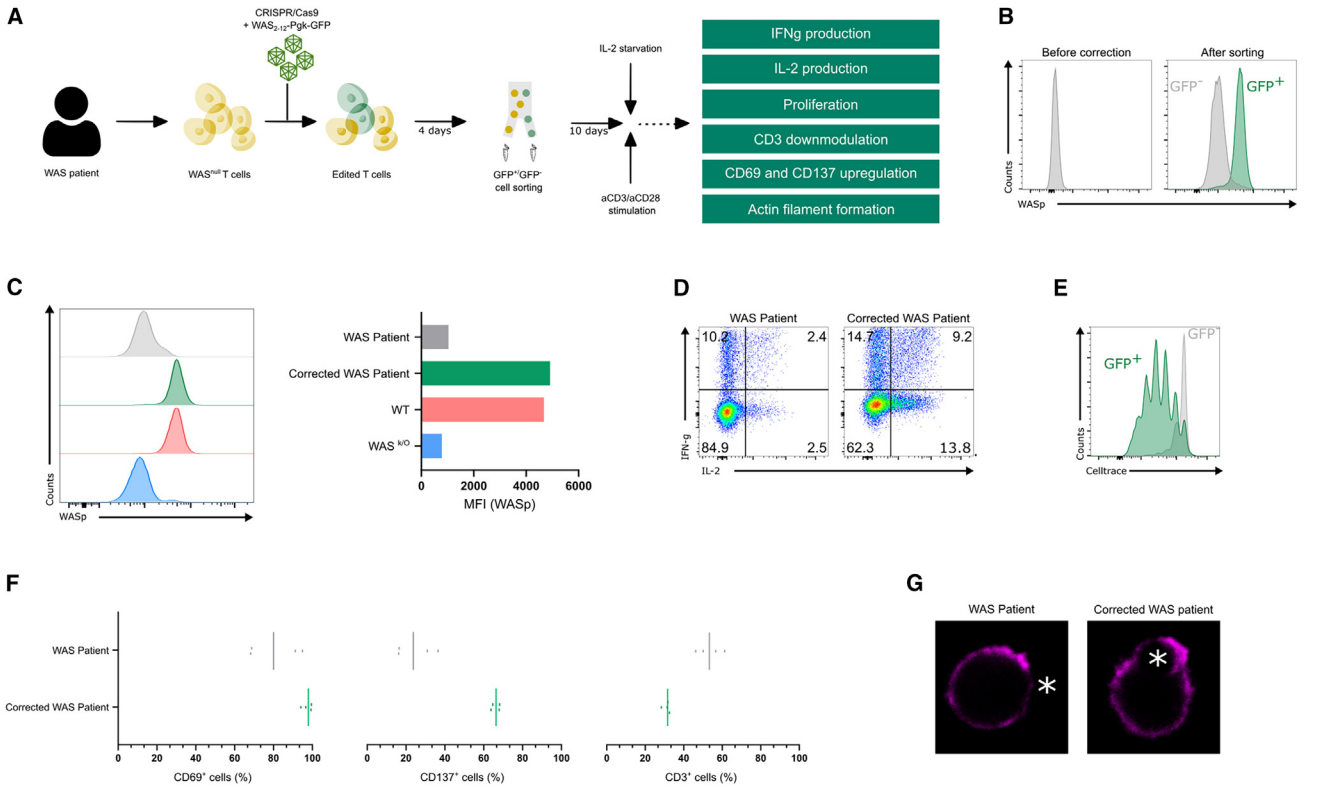

Figure 6. *WAS* TI restores WASp expression and WASp-dependent function to WAS patient T cells

(A) Experimental timeline for editing and functional evaluation of primary WAS T cells.

(B) Pattern of intracellular WASp expression by T cells; FACS histograms of WAS T cells before editing (left panel) and of sorted GFP− and GFP+ cell populations (right panel) after editing.

(C) FACS profile of intracellular WASp expression in T cells (left panel) and mean fluorescence intensity (MFI) (right panel). Color coding is as follows: gray, Uncorrected WAS patient cells; GFP^-; green, Corrected WAS patient cells; GFP^+, pink, Normal, WT WAS cells; blue, WAS knockout cells.

(D) Patterns of IL-2 and IFN-γ expression by αCD3/αCD28-stimulated GFP− Uncorrected WAS Patient (left panel) vs. GFP+ Corrected WAS Patient cells (right panel).

(E) Proliferation of GFP+ and GFP− T cells assessed by CellTrace Violet dye dilution after αCD3/αCD28 stimulation.

(F) Frequency of GFP− Uncorrected WAS Patient or GFP+ Corrected WAS Patient cells expressing CD69, CD137, or CD3 after αCD3/αCD28 stimulation. (D–F) n = 2, experiments from 1 donor.

(G) Detection of actin immune synapse formation in Corrected WAS Patient but not in Uncorrected WAS Patient T cells upon interaction with αCD3/αCD28 coated beads (*).

GFP-expressing cells (Figure 1F). Furthermore, we obtained a lower frequency of $CD34^+$ cells exhibiting TI than we were anticipating (Figure 1G). Performing the similar editing method (with the *$WAS_{2\text{-}12}$-2A-GFP* donor) on a WAS B cell line provided us with cells that could be carefully examined for on-target integration events. For this purpose, we developed ddPCR assays specific for evaluating integration of the upstream and downstream portions of the *$WAS_{2\text{-}12}$-2A-GFP* donor. These assays yielded results for the various cell populations analyzed (RNP+donor, GFP+ sorted, GFP− sorted) in reasonable agreement with the frequency of GFP+ cells as determined by FACS. However, it was only through our development and application of the SMRT-seq with UMI methodology that we were able to obtain a more comprehensive catalog of the types of molecular events resulting from this editing process. The incidence of one of these molecular species (premature crossover) was greatly reduced when we switched from the *$WAS_{2\text{-}12}$-2A-GFP* donor to the *$WAS_{2\text{-}12}$-Pgk-GFP* donor. We attributed this decrease to the incorporation of silent SNPs in exon 2 of the *$WAS_{2\text{-}12}$* transgene in *$WAS_{2\text{-}12}$-Pgk-GFP*. However, we did not formally test this and it is possible that other differences between the *$WAS_{2\text{-}12}$-2A-GFP* and *$WAS_{2\text{-}12}$-Pgk-GFP* donors contributed to or were responsible for this decrease. In any case, our analysis indicated that sorting for GFP+ cells significantly enriched for the desired TI events and depleted those that were undesired.

To limit the occurrence of adverse effects, CRISPR-Cas9-mediated gene therapy should have a safe OT profile with minimal induction of indels, particularly in genomic sequences that could result in undesirable consequences. Using both an *in silico* prediction algorithm and an experimental method for the detection of DSBs, we identified just a single OT site that exhibited indels in CRISPR-Cas9-treated cells at a frequency of >0.1%. Since this OT was located in an intronic region, the likelihood that this OT poses safety concerns would appear to be limited, but this would require more extensive evaluation.

We did not present data that TI CD34$^+$ cells contained multipotent precursors. However, we showed extensive data supporting the notion that TI CD34$^+$ cells contained precursors of myeloid lineage, red blood cell and platelet lineages. We could show *in vitro* as well as *in vivo* B and NK cell precursor activity. In addition, after *in vivo* transplantation, a small but significant percentage of the cells were CD3$^+$ T cells. Finally, TI CD34$^+$ cells were able to engraft in NSG mice and were able to sustain themselves as a prominent population in the bone marrow. Although we did not perform secondary transplants, the fact that TI CD34$^+$ cells were able to maintain themselves and the continued presence of all tested lineages 10 weeks posttransplant is consistent with marking of hematopoietic progenitors that are able to support long-term blood cell production and/or with marking of long-term repopulating HSPCs.

A limitation of this study is the fact that we did not perform TI on actual WAS patients' CD34$^+$ cells. However, we note that the single-nucleotide variants, deletions or insertions responsible for the WAS phenotype are unlikely to affect hybridization of the *WAS* intron 1 gRNA nor the homology arms. Second, we did show that TI works in cord blood as well as adult blood CD34$^+$ cells. Finally, we did show that TI is successful in a WAS B cell line and T cells of WAS patients and was able to revert the phenotype and restore the function. Nevertheless, it remains a possibility that editing of healthy HSPC may not fully recapitulate potential alterations induced in chronic WASp deficiency in human HSPC, finally affecting the editing efficiency or safety in terms of chromosomal damage.

A recent publication reported successful direct targeting of *WAS* exon 1–12 cDNA sequences into *WAS* exon 1.[32] We note that the editing methodology reported in this prior publication, as well as the lentivirus gene addition approach, offers the potential for treatment of all WAS patients. Our approach differs in several respects. Here, we report successful TI of corrective *WAS* sequences specifically into intron 1 of the endogenous *WAS* gene. We deliberately chose this strategy in order to maintain some exon/intron structure—since splicing has been found in transgenic mice to be important for higher levels of transgene expression. We note that the level of restored WASp expression in TI-corrected WAS T cells was indistinguishable from that of the normal, non-WAS control. In addition, *WAS* intron, rather than exon, sequences were selected for nuclease-mediated introduction of the DSBs in order to minimize the potential impact of on-target indels in cells that do not experience successful TI. Although this difference would likely not be relevant for correction of *WAS* mutations having negligible WASp expression, it is unknown whether introduction of NHEJ-induced indels into exon 1 coding sequences would affect the behavior of expressed mutant WASp.

A further difference in our approach was the inclusion of a selectable reporter (in this case GFP) in addition to the correcting $WAS_{2\text{-}12}$ transgene. In some experiments (Figures 2, 3, and6), we utilized the GFP reporter both to enrich for cells with TI and to deplete those cells that were unmodified, had NHEJ-induced indels, or had undergone premature crossover, for example. We note that the combination of methodologies we employed to detail the various consequences of editing (i.e., ddPCR at both ends of the integrated cassette, SMRT-seq with UMI) proved invaluable in cataloging the molecular species comprising the GFP+ and GFP− populations. In principle, the GFP reporter utilized here could be replaced with a surface-expressed marker (e.g., truncated nerve growth factor receptor) for selective transplantation of edited cells into WAS patients. Although there is *in vivo* selection for *WAS*-corrected lymphoid cells in WAS patients exhibiting somatic reversion[33,34] or treated with gene therapy,[10] the selection pressure does not extend to the non-lymphoid lineages. Our future studies will focus on assessing the advantages of delivering only cells pre-selected for correction rather than the total bulk population of corrected and uncorrected cells.

MATERIALS AND METHODS

Sources of human cells

Male donor cord blood samples were obtained from the Hematopoietic Cell Biobank of Ghent University Hospital or the Cord Blood Bank of MD Anderson, University of Texas. Human subject review was performed by University of Texas Health Science Center Committee for the Protection of Human Subjects and the Medical Ethical Committee of the Ghent University Hospital. Male adult mobilized peripheral blood obtained by apheresis, was obtained from the Hematopoietic Cell Biobank of Ghent University Hospital. Peripheral blood of WAS patients was collected following guidelines of the Medical Ethical Committee of the Ghent University Hospital under informed consent in accordance with the Declaration of Helsinki.

gRNAs targeting WAS intron 1 or exon 2

The *WAS*-specific gRNAs (intron 1: 5′ CATGACAGTCATGGGCC CAA 3'; exon 2: 5′ CTGGACCAAGGAGCATTGTG 3′) were purchased as a chemically modified nucleic acid containing a 2-O-methyl and 3′phosphorothioate internucleotide linkage at the first three bases (5′ end) and last three bases (3′ end) (Synthego, Redwood City, CA or Integrated DNA Technologies, Coralville, IA).

Quantification of on-target donor integration by ddPCR

We developed a probe-based ddPCR assay that can quantify the levels of KI at LHA or RHA integration junctions (Figure S1). Probe-based reaction mixes were prepared with 15 ng genomic DNA template, 1× ddPCR Supermix for Probes (Bio-Rad), 900 nM target primers, 250 nM target probes, 900 nM RPP30 reference primers, 250 nM RPP30 reference probes and 10 U BamHI-HF restriction enzyme in each 20 μL reaction mix. To quantify KI at LHA and RHA, two ddPCR reactions were run simultaneously for each sample in technical replicates. The cycling protocol consisted of restriction enzyme digestion (10 min at 37°C), enzyme activation (10 min at 95°), 45 cycles of denaturation (30 s at 94°C), annealing (30 s at 57°C), and extension (2 min at 72°C), followed by enzyme deactivation (10 min at 98°C) and hold (4°C). Since two copies of RPP30 genomic sequences are present in a single diploid human cell, the WAS allele count (cell count) in a sample can be calculated as half of the total number of RPP30 copies per sample.

We also developed an Evagreen-based ddPCR assay that can quantify the frequency of premature crossover relative to the CACNA1C nontargeted reference. A primer pair with forward primer binding upstream the LHA and reverse primer binding at splice acceptor (SA) sequence was used to quantify the total rate of integration at LHA, including LHA KI and premature crossover alleles. The frequency of premature crossover was calculated by subtracting the frequency of LHA KI from the total rate of integration at LHA. The reaction mixes were prepared with 15 ng of gDNA templates, 1× ddPCR Evagreen Supermix (Bio-Rad), 200 nM target or nontargeted reference primers, and 10 U of Hind III–HF restriction enzyme in each 20 μL of reaction mix. PCR was performed according to the manufacturer's cycling protocol. The primer and probe sequences for ddPCR assays are provided in Table S2.

Isolation of CD34$^+$ HSPCs

Mononuclear cells were isolated from umbilical cord blood or peripheral blood by density gradient centrifugation (density of 1,077). Subsequently, CD34$^+$ HSPCs were purified using the human CD34 MicroBead kit (Miltenyi Biotec, Cologne, Germany) according to manufacturer instructions with minor alterations. The labeled cell suspension was passed 2–3 times through the magnet to obtain a purity of >95%. Sample purity was assessed on a BD LSR2 with anti-human CD34 APC and CD45 AmCyan (both BD Biosciences, Franklin Lakes, NJ or BioLegend, San Diego, CA) and anti-human CD3 PEcy7 (BiolLgend).

Cell culture conditions

CD34$^+$ HSPCs were incubated in StemSpan SFEM supplemented with TPO, SCF, FLT3-L, IL-6 (all at 100 ng/mL), StemRegenin 1 (0.75 μM) and UM171 (35nM) (all from Stemcell Technologies, Vancouver, Canada except for IL-6: Tebu-Bio, Le Perray-en-Yvelines, France) and cultured at 37°C in humidified air/5% CO_2 for *in vitro* experiments or at 5% O_2 90% N_2 5% CO_2 for *in vivo* experiments. Activated T cells were produced as follows: peripheral blood mononuclear cells were stimulated with 10μL Immunocult Human CD3/CD28/CD2 T cell activator (STEMCELL Technologies, Vancouver, Canada) in the presence of 10 ng/mL IL-2 in complete IMDM (cIMDM). cIMDM is IMDM (Gibco, Invitrogen, Waltham, MA) supplemented with 10% fetal calf serum (FCS) (Gibco, Invitrogen), 2 mM L-glutamine (Gibco, Invitrogen), 100 IU/mL penicillin (Gibco, Invitrogen) and 100 IU/mL streptomycin (Gibco, Invitrogen). The percentage of CD3$^+$ T cells was determined on a BD LSR2 with anti-human CD3 Pe-cy7 and CD45 amcyan. MS5 cells were passaged in MEMα supplemented with 10% FCS, 100 IU/mL penicillin and 100 IU/mL streptomycin (complete MEMα, cMEMα). EL08-1D2 cells were cultured at 32°C on 0.1% gelatin-coated plates in 50% Myelocult M5300 medium (STEMCELL Technologies), 35% α-MEM and 15% heat-inactivated FCS, supplemented with penicillin (100 U/mL), streptomycin (100 μg/mL), L-glutamine (2 mM), and β-mercaptoethanol (10 μM) (Merck, Darmstadt, Germany). EBV-transformed WAS mutant (GM21868) or control B cell lines (GM22647) (Coriell Institute for Medical Research, Camden, NJ) were cultured in RPMI 1640 (Corning, Manassas, VA) supplemented with 15% HyClone Characterized Fetal Bovine Serum (Cytiva Life Sciences, Marlborough, MA) per Coriell Institute protocol.

Construction and production of AAV-6 donor vectors

Donor templates and AAV6 production are based on the protocol as described by Bak et al. with minor modifications.[21] In short, all donor templates were cloned into pAAV-MCS (Agilent Technologies, Santa Clara, CA). The length of left and right homology arms were 814 and 776 bp, respectively, for *PGK-GFP*, and 512 and 488 bp, respectively, for $WAS_{2\text{-}12}$, $WAS_{2\text{-}12}$*-PGK-GFP*, and $WAS_{2\text{-}12}$*-2A-GFP*. The *WAS* cDNA was preceded by a synthetic splice acceptor sequence and followed by a bovine rowth hormone poly(A) sequence. For the $WAS_{2\text{-}12}$*-pgk-GFP* donor, the $WAS_{2\text{-}12}$ cDNA sequences contained four silent mutations in exon 2 and three silent mutations in exon 3 to reduce the possibility of premature crossover events during HDR. AAV6 vector particles were either produced commercially (Vigene Biosciences, Rockville, MD) or by co-transfection of HEK293T cells with the donor construct and the pDGM6 Rep/Cap helper plasmid (Plasmid Factory, Bielefeld, Germany). After 72 h culture, cells and supernatant were harvested and pelleted. AAV lysis buffer was added and the suspension was submitted to three freeze-thaw cycles. After the third thaw, benzonase (200 U/mL final concentration) (Merck, Darmstadt, Germany) was added and the suspension was incubated in a 37°C water bath for 1 h. After centrifugation, the supernatant was submitted to iodixanol gradient purification as described by Bak et al..[21] The titer of the viral particles was determined by quantitative PCR using primers complementary to eGFP present in $WAS_{2\text{-}12}$*-PGK-GFP* and $WAS_{2\text{-}12}$*-2A-GFP* or using the AAVpro Titration Kit (Takara Bio USA, San Jose, CA).

Gene editing of HSPCs and T cells

CD34$^+$ HSPCs, pre-cultured for 48 h for *in vitro* experiments or O/N for *in vivo* experiments, were subjected to nucleofection according to the protocol of Bak et al..[21] In short, Alt-R S.p. HiFi Cas9 nuclease (Integrated DNA Technologies) was complexed with the sgRNA(s) (molar ratio 1:2.5) for 10 min at 25°C to form the RNP. Cells (2×10^5 to 1×10^6) were pelleted, resuspended in supplemented Nucleofection Solution (Lonza, Pearland, TX) and subsequently mixed with the RNP. The suspension was transferred to a cuvette and nucleofected using the Lonza 4D and the DZ100 program. After electroporation, the cells were transferred to a 48-well in cIMDM and immediately transduced for 5 h with 10^5 viral genomes (VG)/cell AAV6 donor constructs. Viability after electroporation was between 60% and 80%. Activated T cells were harvested 72 h after stimulation and nucleofected. A total of 4×10^5 cells were pelleted, resuspended in supplemented Nucleofection Solution and mixed with the RNP. Using the Lonza 4D and the EH100 program, the cells were nucleofected. After nucleofection, the cells were transferred to a 48-well containing cIMDM with 10 ng/mL IL-2 and immediately transduced with 10^5 VG/cell AAV6 donor constructs. After overnight incubation, the viral particles were washed away. Four days after editing, T cells were labeled with CD3-PEcy7 for 30 min at 4°C. GFP+ and GFP− T cells were separately sorted and cultured. After 7 days, cells were

expanded onto feeder cells using the protocol by De Munter et al. until sufficient cells were present to perform functional assays.

OT identification

Bioinformatic prediction of potential OT sites for gRNA targeting intron 1 of *WAS* was carried out using the web-based tool COSMID[16] allowing for up to three mismatches or with up to two mismatches and an insertion or deletion allowed in the 19 PAM proximal bases. The Homo sapiens genome assembly GRCh38/hg38 genome build was used as a reference. GUIDE-seq[17,18] was used for experimental identification of potential OT sites, which relies on capture of a dsODN into DSBs to identify CRISPR-induced OT activities in the genome globally by sequencing. In brief, a WAS intron targeting gRNA/HiFi Cas9 RNP along with a iGUIDE dsDNA tag was nucleofected into normal (non-WAS) male CB $CD34^+$ cells. Genomic DNA was extracted 4 days post electroporation and subjected to enzymatic fragmentation, end repair, A-tailing, and Y-adapter ligation according to the manufacturer's instructions (NEBNext Ultra II FS DNA Library Prep), followed by two rounds of discovery PCRs. Libraries were loaded into a 300-cycle version 2 Illumina kit, and run on a MiSeq (Illumina, San Diego, CA). Sequences were processed using the iGUIDE pipeline publicly available on GitHub (https://github.com/cnobles/iGUIDE). GRCh38/hg38 was used as a reference genome.

Quantification of on-target and OT activity by deep sequencing

WAS intron 1 targeting gRNA/HiFi Cas9 RNP was nucleofected into normal (non-WAS) male CB $CD34^+$ cells. DNA flanking the gRNA on- and OT sites (identified by COSMID and GUIDE-seq) was amplified using locus-specific primers followed by a second PCR to introduce Illumina sequencing adaptors and sample barcodes. The library preparation and sample loading were performed as described previously[35] CRISPR-Cas9 genome editing outcomes from deep sequencing data were analyzed using a CRISPResso2.[36]

In vitro differentiation of edited $CD34^+$ HSPCs into hematopoietic progeny

Erythrocyte and megakaryocyte lineage

HSPCs (3.5×10^3) were cultured in 96-well U-bottom plates in cMEMα supplemented with 2 mM L-glutamine, 5 ng/mL SCF, 50 ng/mL TPO, and 5 ng/mL EPO. Once per week new medium was added and cells were passaged as needed. After 14 days, megakaryocyte lineage cells differentiation was assessed by staining with CD41 PEcy7 and CD42b APC. Generation of erythrocyte lineage cells was evaluated by staining with CD71 APC-cy7and CD235 PE.

B lineage cells

HSPCs (3.5×10^3) were cultured on a monolayer of MS5 in cIMDM supplemented with 10% heat-inactivated human AB serum (Biowest, Nuaillé, France) (hIMDM), 20 ng/mL SCF and 20 ng/mL hIL-7 (Miltenyi Biotec, Bergisch Gladbach, Germany). Once a week, the cells were transferred to a fresh MS5 monolayer. Differentiation of B cells was assessed after 3 weeks of culture by staining with anti-human CD20 AF-700 and CD19 APC.

Myeloid cells

HSPCs (3.5×10^3) were cultured on a monolayer of MS5 in hIMDM supplemented with 20 ng/mL Flt3-L, SCF, and TPO and 10 ng/mL GM-CSF and G-CSF (both from Gentaur Europe, Kampenhout, Belgium). Once a week, cells were transferred to a fresh monolayer of MS5 cells. Myeloid differentiation was evaluated at 3 weeks by staining with CD14 PB, CD4 PercpCy5.5, CD15 PE, and HLA-DR APC-cy7 for the detection of monocytes and neutrophils.

NK cell differentiation

NK cells were generated according to the protocol by Persyn et al.. In brief, HPCs were plated on mitomycin C-inactivated murine embryonic liver cell line EL08-1D2 in NK co-culture medium (DMEM and HAM F-12 nutrient mixture [2:1 ratio], supplemented with 2 mM L-glutamine, 100 IU/mL penicillin, and 100 IU/mL streptomycin, 10 mM sodium pyruvate, 20% heat-inactivated human AB serum, 24 µM β-Mercaptoethanol, 20 µg/mL ascorbic acid, 50 µM ethanolamine and 50 ng/mL sodium selenite [all from Sigma-Aldrich, Burlington, MA]) 5 ng/mL IL-3, 20 ng/mL IL-7 and SCF, and 10 ng/mL IL-15 (Miltenyi Biotec) and Flt3-L were added. One week later, medium was added (except for the IL-3). At day 14, cells were transferred to freshly inactivated EL08 cells. After 4 weeks of culture, differentiation in NK cells was evaluated by staining with CD94 PE and CD56 BV421.

Transplantation of edited $CD34^+$ HSPCs into immunodeficient mice

Mouse experiments were performed in accordance with the guidelines of the Ethical Committee for Experimental Animals at the Faculty of Medicine and Health Sciences of Ghent University (ref. no. ECD17/05, Ghent, Belgium). *In vivo* experiments were conducted according to the protocol of Bak et al.[21] (NSG pup recipients) or Rai et al.[32] (adult NSG recipient mice). NOD.Cg-Prkdc^{scid} Il2rg^{tm1Wjl}/SzJ (NSG) pups (max 3 days old) or NSG adult mice (6–7 weeks old) were sublethally irradiated 8–24 h before transplantation with 100 or 200 cGy, respectively. $CD34^+$ cells were isolated from either fresh cord blood or thawed apheresed peripheral blood and cultured overnight at 5% O_2. Cells were then electroporated according to our standard protocol and immediately injected into NSG mice. A total of 3×10^5 gene edited or mock edited HSPC-C were delivered via intrahepatic injection to pups; 3×10^5 gene edited or mock edited HSPC-A cells were delivered intravenously to adults. After 10–11 week, the mice were sacrificed, and the bone marrow, spleen, and thymus were harvested. Single-cell suspensions were generated from these organs as described previousy.[37–39] The presence of human stem/progenitor ($CD34^+$), B ($CD20^+$), T ($CD3^+$), and NK cells ($CD56^+$), granulocytes (FSC-A and SSC-A) and monocytes ($CD33^+$) were analyzed using flow cytometry.

Flow cytometric analysis and cell sorting

Analysis of samples was performed on an LSR2 (Becton Dickinson), and sorting was performed either on an ARIA (Becton Dickinson), FACS Melody (Becton Dickinson), or Fusion-instrument (Becton Dickinson). Doublets were excluded from the analysis based on

FSC-H and FSC-A and dead cells were gated out using PI or Life/Death-amcyan. Labeled antibodies were obtained from BioLegend): CD3 PEcy7, CD3 APC-cy7, CD4 PerCPcy5.5, CD5-PE, CD8 amcyan, CD8 APC-Cy7, CD19 PB, CD15 PE, CD19 APC, CD20 AF-700, CD20 APC, CD27 APC-Cy7, CD33 PE, CD34 PerCPcy5.5, CD34 APC, CD41 PEcy7, CD42b APC, CD45 amcyan, CD45 PEcy7, CD56 BV421, CD69 PEcy7, CD71 APC-Cy7, CD94 PE, CD137 PE, CD235PE, HLA-DR APC-Cy7, IFN-γ PE, IL-2 PB; Thermo Fisher Scientific: CellTrace Violet Cell Proliferation Kit and Santa Cruz Biotechnology: WASp AF647.

Editing and functional studies of human WAS T cells

All functional assays are based on the protocols described in Dupré et al.[12] with minor alterations.

Cytokine assay

NTC flat bottom 96-well plate wells were coated overnight with OKT3 mAb (ATCC, Manassas, VA) at the indicated concentrations. The next day, excess OKT3 was removed. A total of 5×10^4 cells were added in cIMDM with 10 ng/mL aCD28 (BD Biosciences, Franklin Lakes, NJ). Two hours later, brefeldin A Golgiplug (BD Biosciences) was added in a 1/750 final dilution. After an additional 4 h, T cells were harvested, stained for membrane markers, and were subsequently fixed and permeabilized using the Cytofix/Cytoperm Kit (BD Biosciences) before intracellular staining for IFN-γ, IL-2, and WASp.

Stimulation assay

The same protocol was used as for the cytokine assay except for the addition of brefeldin A. After 6 h of stimulation, cells were stained for CD3, CD4, CD8, CD69, CD137. After membrane staining, cells were fixated and permeabilized and subsequently stained for WASp+.

Proliferation assay

GFP+ and GFP− cells were labeled with the CellTrace Violet Cell Proliferation Kit according to manufacturing protocol. In brief, 10^6 cells were labeled with 1 μL of a Celltrace working solution (lyophilized Celltrace resuspended in 200 μL DMSO) in 1 mL PBS. A total of 50,000 labeled cells were then added to OKT3-coated 96-wells together with 10 ng/mL aCD28 for 6 days. At day 3, new cIMDM was added. Cells were harvested and stained with CD3, CD4, CD8 and for WASp after fixation and permeabilization using the Cytofix/Cytoperm Kit.

Actin filament formation assay

Cells (1.5×10^4) are incubated with Dynabeads Human T-Activator CD3/CD28 (Gibco) at a 2:1 bead-to-cell ratio for 20 min at 37°C. Cells are gently washed and transferred to poly-L-lysine-coated (0.1 mg/mL) plates. After a 20 min incubation, 80 μL of a 4% paraformaldehyde solution was added to each well and incubated for 15 min at room temperature (RT). The wells were washed with ice-cold PBS in TrypLE and 80 μL of 0.25% Triton X-100 PBS was added for 15 min. The supernatant was removed and cells were washed in PBS 1% BSA. Subsequently, the cells were incubated with 1% BSA, 22.5 mg/mL glycine in PBS for 1 h. Alexa Fluor 555-conjugated phalloidin (Thermo Fisher Scientific) was added to each well in a 1/100 dilution at 4°C on a shaker. After overnight incubation, cells were washed in PBS and DAPI (1/5,000 dilution) was added for 10 min at RT. Finally, DAPI was washed away with PBS. Images were acquired with a Leica SP8 confocal laser scanning microscope (Leica Microsystems, Wetzlar, Germany).

Correction of human WAS B cell line

Lentivirus construction, production, and transduction

The lentiviral construct was based on the pRRLSIN.cPPT.WPRE vector, into which was cloned the *W1.6-WAS$_{1\text{-}12}$-2A-GFP* insert to yield pRRLSIN.cPPT.W1.6-WAS$_{1\text{-}12}$-2A-GFP.WPRE. W1.6 is the 1.6 kb *WAS* promoter sequence (from D.J. Rawlings, Addgene, no. 36250) and the *WAS$_{1\text{-}12}$-2A-GFP* expression cassette contains the *WAS* cDNA (exons 1–12) fused to eGFP via 2A sequences. 293T packaging cells (Takara Bio USA) were transfected using P3000 reagent (Thermo Fisher Scientific), the aforementioned vector, pCMV-dR8.91 (Creative Biogene, Shirley NY), and pCMV-VSV-G (Addgene). After 18 h, the media was replaced then collected after 48 h. The supernatant was concentrated by mixing 20% sucrose in HBSS and the supernatant collected previously. This mixture was then subjected to ultracentrifugation at 27,000 rpm for 2 h at 4°C. After removing the supernatant and drying, 200 μL of PBS was added. Viral titer was determined by seeding 75,000 cells into wells of a 6-well plate and incubating overnight. Lentiviral dilutions of 1.5 mL total volume into DMEM with 10 μg/mL polybrene were prepared (1:10, 1:25, 1:50, 1:75, 1:100). The cells were counted and incubated for 48 h. The media was aspirated and replaced with 1 mL PBS. In wells that contained less than 40% fluorescent cells, the fraction of fluorescent cells was calculated by employing the equation, $T = (N * F * D)/V_T$ where N is the number of cells transduced, F is the fraction of fluorescent cells, D is the dilution factor, V_T is the transduction volume, and T is the titer (TU/mL). The EBV-transformed WAS B cell line (GM21868) (Coriell Institute for Medical Research) was transduced according to Cold Spring Harbor Protocol for Lentiviral Transduction (2007) with a virus dose selected to obtain single-cell-derived clones with one integrated lentiviral copy per cell. Flow cytometric analysis on a BD FACS Melody was used to assess GFP expression and AAV-transduced GFP+ cells were sorted; lentiviral-transduced cells were single-cell sorted for GFP and cultured for clonal isolation.

B cell editing

B cells (2×10^5) were nucleofected in P3 primary cell buffer (Lonza, Basel, Switzerland) with Alt-R S.p. HiFi Cas9 nuclease and sgRNA (Integrated DNA Technologies), as described above, using program EO-117. Immediately post-nucleofection, cells were transduced with 10^5 VG/Cell of AAV6 *WAS$_{2\text{-}12}$-2A-GFP*. After 5 h, the medium was refreshed. Flow cytometric analysis on a BD FACS Melody was used to sort GFP-expressing cells, which were then expanded in bulk.

Western blotting for detection of WASp

Protein preparation

Protein samples were extracted from cells via incubation with RIPA Lysis buffer (Millipore, Burlington, MA) containing protease inhibitor

(Roche, Burlington, MA). Protein was analyzed via colorimetric BSA assay (Thermo Fisher Scientific, Waltham, MA).

Electrophoresis

Samples were prepared for gel electrophoresis by addition of LDS sample buffer (Thermo Fisher Scientific), and sample reducing agent (Thermo Fisher Scientific). Samples were run on NuPage 7% Tris-Acetate gels (Thermo Fisher Scientific) in Tris-Acetate SDS running buffer (Thermo Fisher Scientific) plus antioxidant (Thermo Fisher Scientific). Electrophoresis was first performed at 100 V for the first 10 min then run at 150 V for 1 h.

Transfer

Western blotting followed the Thermo Fisher Scientific protocol with the modification that the transfer was performed at 45 V for 2.5 h. All reagents listed in the protocol for nitrocellulose membrane transfer remain the same.

Antibody incubation

Membrane was blocked with 5% milk (LabScientific, Danvers, MA) for 1 h. After blocking, the membrane was incubated with either 1:5,000 anti-WASp-HRP (B-9) (Santa Cruz Biotechnology, Dallas, TX) or 1:10,000 anti-β Actin-HRP (C4) (SCBT) overnight at 4°C.

Detection

Membranes were washed using 1× Tris-Buffered Saline (Thermo Fisher Scientific) and Amersham ECL Detection reagent (Cytiva Life Sciences) was used to prepare the membrane for exposure on Amersham Hyperfilm MP (Cytiva Life Sciences).

Statistical analysis

All calculations and statistical analyses were performed using GraphPad Prism software version 8.4.3 (GraphPad, San Diego, CA). The statistical tests used are indicated in figure legends. p-values less than 0.05 were considered to be statistically significant.

DATA AND CODE AVAILABILITY

All data needed to evaluate the conclusions in the paper are present in the paper and/or the supplemental materials. Illumina sequencing data are accessible at the Sequence Read Archive (SRA) under accession number PRJNA805265.

SUPPLEMENTAL INFORMATION

Supplemental information can be found online at https://doi.org/10.1016/j.omtm.2024.101208.

ACKNOWLEDGMENTS

Funding provided by the C. Harold and Lorine G. Wallace Distinguished University Chair (to B.R.D.), the National Institutes of Health (R01HL152314 and R01HL169761 to G.B.), FWO grant G036717N (to B.V.), and FWO Doctoral grant strategic basic research 1S14328N (to M.P.).

AUTHOR CONTRIBUTIONS

M.P., J.M.A., S.H.P., C.Q.L., H.X., L.S., and C.L. performed the experimental studies described in this article. F.H. provided the WAS patient peripheral blood sample. E.J.S. provided cord blood. G.B., S.H.P., B.V., M.P., B.R.D., and J.M.A. were responsible for design of the experimental work. G.B., B.V., M.P., and B.R.D. were responsible for overseeing both the experimental work and the writing of the manuscript.

DECLARATION OF INTERESTS

The authors declare no competing interests.

REFERENCES

1. Jin, Y., Mazza, C., Christie, J.R., Giliani, S., Fiorini, M., Mella, P., Gandellini, F., Stewart, D.M., Zhu, Q., Nelson, D.L., et al. (2004). Mutations of the Wiskott-Aldrich Syndrome Protein (WASP): hotspots, effect on transcription, and translation and phenotype/genotype correlation. Blood *104*, 4010–4019. https://doi.org/10.1182/blood-2003-05-1592.

2. Massaad, M.J., Ramesh, N., and Geha, R.S. (2013). Wiskott-Aldrich syndrome: a comprehensive review. Ann. N. Y. Acad. Sci. *1285*, 26–43. https://doi.org/10.1111/nyas.12049.

3. Ochs, H.D., and Thrasher, A.J. (2006). The Wiskott-Aldrich syndrome. J. Allergy Clin. Immunol. *117*, 725–739. quiz 739. https://doi.org/10.1016/j.jaci.2006.02.005.

4. Rivers, E., and Thrasher, A.J. (2017). Wiskott-Aldrich syndrome protein: Emerging mechanisms in immunity. Eur. J. Immunol. *47*, 1857–1866. https://doi.org/10.1002/eji.201646715.

5. Sun, X., Wei, Y., Lee, P.P., Ren, B., and Liu, C. (2019). The role of WASp in T cells and B cells. Cell. Immunol. *341*, 103919. https://doi.org/10.1016/j.cellimm.2019.04.007.

6. Ngoenkam, J., Paensuwan, P., Wipa, P., Schamel, W.W.A., and Pongcharoen, S. (2021). Wiskott-Aldrich Syndrome Protein: Roles in Signal Transduction in T Cells. Front. Cell Dev. Biol. *9*, 674572. https://doi.org/10.3389/fcell.2021.674572.

7. Blundell, M.P., Worth, A., Bouma, G., and Thrasher, A.J. (2010). The Wiskott-Aldrich syndrome: The actin cytoskeleton and immune cell function. Dis. Markers *29*, 157–175. https://doi.org/10.3233/DMA-2010-0735.

8. Cotta-de-Almeida, V., Westerberg, L., Maillard, M.H., Onaldi, D., Wachtel, H., Meelu, P., Chung, U.I., Xavier, R., Alt, F.W., and Snapper, S.B. (2007). Wiskott Aldrich syndrome protein (WASP) and N-WASP are critical for T cell development. Proc. Natl. Acad. Sci. USA *104*, 15424–15429. https://doi.org/10.1073/pnas.0706881104.

9. Braun, C.J., Boztug, K., Paruzynski, A., Witzel, M., Schwarzer, A., Rothe, M., Modlich, U., Beier, R., Göhring, G., Steinemann, D., et al. (2014). Gene therapy for Wiskott-Aldrich syndrome–long-term efficacy and genotoxicity. Sci. Transl. Med. *6*, 227ra33. https://doi.org/10.1126/scitranslmed.3007280.

10. Aiuti, A., Biasco, L., Scaramuzza, S., Ferrua, F., Cicalese, M.P., Baricordi, C., Dionisio, F., Calabria, A., Giannelli, S., Castiello, M.C., et al. (2013). Lentiviral hematopoietic stem cell gene therapy in patients with Wiskott-Aldrich syndrome. Science *341*, 1233151. https://doi.org/10.1126/science.1233151.

11. Magnani, A., Semeraro, M., Adam, F., Booth, C., Dupré, L., Morris, E.C., Gabrion, A., Roudaut, C., Borgel, D., Toubert, A., et al. (2022). Long-term safety and efficacy of lentiviral hematopoietic stem/progenitor cell gene therapy for Wiskott-Aldrich syndrome. Nat. Med. *28*, 71–80. https://doi.org/10.1038/s41591-021-01641-x.

12. Dupré, L., Trifari, S., Follenzi, A., Marangoni, F., Lain de Lera, T., Bernad, A., Martino, S., Tsuchiya, S., Bordignon, C., Naldini, L., et al. (2004). Lentiviral vector-mediated gene transfer in T cells from Wiskott-Aldrich syndrome patients leads to functional correction. Mol. Ther. *10*, 903–915. https://doi.org/10.1016/j.ymthe.2004.08.008.

13. Hacein-Bey Abina, S., Gaspar, H.B., Blondeau, J., Caccavelli, L., Charrier, S., Buckland, K., Picard, C., Six, E., Himoudi, N., Gilmour, K., et al. (2015). Outcomes following gene therapy in patients with severe Wiskott-Aldrich syndrome. JAMA *313*, 1550–1563. https://doi.org/10.1001/jama.2015.3253.

14. Chu, J.I., Henderson, L.A., Armant, M., Male, F., Dansereau, C.H., MacKinnon, B., Burke, C.J., Cavanaugh, M.E., London, W.B., Barlan, I.B., et al. (2015). Gene Therapy Using a Self-Inactivating Lentiviral Vector Improves Clinical and Laboratory Manifestations of Wiskott-Aldrich Syndrome. Blood *126*, 260. https://doi.org/10.1182/blood.V126.23.260.260.

15. Laskowski, T.J., Van Caeneghem, Y., Pourebrahim, R., Ma, C., Ni, Z., Garate, Z., Crane, A.M., Li, X.S., Liao, W., Gonzalez-Garay, M., et al. (2016). Gene Correction of iPSCs from a Wiskott-Aldrich Syndrome Patient Normalizes the Lymphoid Developmental and Functional Defects. Stem Cell Rep. *7*, 139–148. https://doi.org/10.1016/j.stemcr.2016.06.003.

16. Cradick, T.J., Qiu, P., Lee, C.M., Fine, E.J., and Bao, G. (2014). COSMID: A Web-based Tool for Identifying and Validating CRISPR/Cas Off-target Sites. Mol. Ther. Nucleic Acids *3*, e214. https://doi.org/10.1038/mtna.2014.64.

17. Nobles, C.L., Reddy, S., Salas-McKee, J., Liu, X., June, C.H., Melenhorst, J.J., Davis, M.M., Zhao, Y., and Bushman, F.D. (2019). iGUIDE: an improved pipeline for analyzing CRISPR cleavage specificity. Genome Biol. *20*, 14. https://doi.org/10.1186/s13059-019-1625-3.

18. Tsai, S.Q., Zheng, Z., Nguyen, N.T., Liebers, M., Topkar, V.V., Thapar, V., Wyvekens, N., Khayter, C., Iafrate, A.J., Le, L.P., et al. (2015). GUIDE-seq enables genome-wide profiling of off-target cleavage by CRISPR-Cas nucleases. Nat. Biotechnol. *33*, 187–197. https://doi.org/10.1038/nbt.3117.

19. De Ravin, S.S., Reik, A., Liu, P.Q., Li, L., Wu, X., Su, L., Raley, C., Theobald, N., Choi, U., Song, A.H., et al. (2016). Targeted gene addition in human CD34(+) hematopoietic cells for correction of X-linked chronic granulomatous disease. Nat. Biotechnol. *34*, 424–429. https://doi.org/10.1038/nbt.3513.

20. Wang, J., Exline, C.M., DeClercq, J.J., Llewellyn, G.N., Hayward, S.B., Li, P.W.L., Shivak, D.A., Surosky, R.T., Gregory, P.D., Holmes, M.C., and Cannon, P.M. (2015). Homology-driven genome editing in hematopoietic stem and progenitor cells using ZFN mRNA and AAV6 donors. Nat. Biotechnol. *33*, 1256–1263. https://doi.org/10.1038/nbt.3408.

21. Bak, R.O., Dever, D.P., and Porteus, M.H. (2018). CRISPR/Cas9 genome editing in human hematopoietic stem cells. Nat. Protoc. *13*, 358–376. https://doi.org/10.1038/nprot.2017.143.

22. Karst, S.M., Ziels, R.M., Kirkegaard, R.H., Sørensen, E.A., McDonald, D., Zhu, Q., Knight, R., and Albertsen, M. (2021). High-accuracy long-read amplicon sequences using unique molecular identifiers with Nanopore or PacBio sequencing. Nat. Methods *18*, 165–169. https://doi.org/10.1038/s41592-020-01041-y.

23. Park, S.H., Cao, M., Pan, Y., Davis, T.H., Saxena, L., Deshmukh, H., Fu, Y., Treangen, T., Sheehan, V.A., and Bao, G. (2022). Comprehensive analysis and accurate quantification of unintended large gene modifications induced by CRISPR-Cas9 gene editing. Sci. Adv. *8*, eabo7676. https://doi.org/10.1126/sciadv.abo7676.

24. Dever, D.P., Bak, R.O., Reinisch, A., Camarena, J., Washington, G., Nicolas, C.E., Pavel-Dinu, M., Saxena, N., Wilkens, A.B., Mantri, S., et al. (2016). CRISPR/Cas9 beta-globin gene targeting in human haematopoietic stem cells. Nature *539*, 384–389. https://doi.org/10.1038/nature20134.

25. Zhu, Q., Watanabe, C., Liu, T., Hollenbaugh, D., Blaese, R.M., Kanner, S.B., Aruffo, A., and Ochs, H.D. (1997). Wiskott-Aldrich syndrome/X-linked thrombocytopenia: WASP gene mutations, protein expression, and phenotype. Blood *90*, 2680–2689.

26. Lemahieu, V., Gastier, J.M., and Francke, U. (1999). Novel mutations in the Wiskott-Aldrich syndrome protein gene and their effects on transcriptional, translational, and clinical phenotypes. Hum. Mutat. *14*, 54–66. https://doi.org/10.1002/(SICI)1098-1004(1999)14:1<54::AID-HUMU7>3.0.CO;2-E.

27. Lutskiy, M.I., Park, J.Y., Remold, S.K., and Remold-O'Donnell, E. (2008). Evolution of highly polymorphic T cell populations in siblings with the Wiskott-Aldrich Syndrome. PLoS One *3*, e3444. https://doi.org/10.1371/journal.pone.0003444.

28. Canaj, H., Hussmann, J.A., Li, H., Beckman, K.A., Goodrich, L., Cho, N.H., Li, Y.J., Santos, D.A., McGeever, A., Stewart, E.M., et al. (2019). Deep Profiling Reveals Substantial Heterogeneity of Integration Outcomes in CRISPR Knock-In Experiments. Preprint at bioRxiv. https://doi.org/10.1101/841098.

29. Giorgi, M.D., Park, S.H., Castoreno, A., Cao, M., Hurley, A., Saxena, L., Chuecos, M.A., Walkey, C.J., Doerfler, A.M., Furgurson, M.N., et al. (2023). In Vivo Expansion of Gene-Targeted Hepatocytes through Transient Inhibition of an Essential Gene. Preprint at bioRxiv. https://doi.org/10.1101/2023.07.26.550728.

30. McCarty, D.M., Young, S.M., Jr., Samulski, R.J., and Samulski, R.J. (2004). Integration of Adeno-Associated Virus (AAV) and Recombinant AAV Vectors. Annu. Rev. Genet. *38*, 819–845. https://doi.org/10.1146/annurev.genet.37.110801.143717.

31. Park, S.H., Cao, M., and Bao, G. (2023). Detection and quantification of unintended large on-target gene modifications due to CRISPR/Cas9 editing. Current Opinion in Biomedical Engineering *28*, 100478. https://doi.org/10.1016/j.cobme.2023.100478.

32. Rai, R., Romito, M., Rivers, E., Turchiano, G., Blattner, G., Vetharoy, W., Ladon, D., Andrieux, G., Zhang, F., Zinicola, M., et al. (2020). Targeted gene correction of human hematopoietic stem cells for the treatment of Wiskott - Aldrich Syndrome. Nat. Commun. *11*, 4034. https://doi.org/10.1038/s41467-020-17626-2.

33. Davis, B.R., and Candotti, F. (2009). Revertant somatic mosaicism in the Wiskott-Aldrich syndrome. Immunol. Res. *44*, 127–131. https://doi.org/10.1007/s12026-008-8091-4.

34. Davis, B.R., Yan, Q., Bui, J.H., Felix, K., Moratto, D., Muul, L.M., Prokopishyn, N.L., Blaese, R.M., and Candotti, F. (2010). Somatic mosaicism in the Wiskott-Aldrich syndrome: molecular and functional characterization of genotypic revertants. Clin. Immunol. *135*, 72–83. https://doi.org/10.1016/j.clim.2009.12.011.

35. Park, S.H., Lee, C.M., and Bao, G. (2022). Identification and Validation of CRISPR/Cas9 Off-Target Activity in Hematopoietic Stem and Progenitor Cells. Methods Mol. Biol. *2429*, 281–306. https://doi.org/10.1007/978-1-0716-1979-7_19.

36. Clement, K., Rees, H., Canver, M.C., Gehrke, J.M., Farouni, R., Hsu, J.Y., Cole, M.A., Liu, D.R., Joung, J.K., Bauer, D.E., and Pinello, L. (2019). CRISPResso2 provides accurate and rapid genome editing sequence analysis. Nat. Biotechnol. *37*, 224–226. https://doi.org/10.1038/s41587-019-0032-3.

37. Filtjens, J., Keirsse, J., Van Ammel, E., Taveirne, S., Van Acker, A., Kerre, T., Taghon, T., Vandekerckhove, B., Plum, J., Van Ginderachter, J.A., and Leclercq, G. (2016). Expression of the inhibitory Ly49E receptor is not critically involved in the immune response against cutaneous, pulmonary or liver tumours. Sci. Rep. *6*, 30564. https://doi.org/10.1038/srep30564.

38. Filtjens, J., Taveirne, S., Van Acker, A., Van Ammel, E., Vanhees, M., Kerre, T., Taghon, T., Vandekerckhove, B., Plum, J., and Leclercq, G. (2013). Abundant stage-dependent Ly49E expression by liver NK cells is not essential for their differentiation and function. J. Leukoc. Biol. *93*, 699–711. https://doi.org/10.1189/jlb.0812378.

39. Van Acker, A., Gronke, K., Biswas, A., Martens, L., Saeys, Y., Filtjens, J., Taveirne, S., Van Ammel, E., Kerre, T., Matthys, P., et al. (2017). A Murine Intestinal Intraepithelial NKp46-Negative Innate Lymphoid Cell Population Characterized by Group 1 Properties. Cell Rep. *19*, 1431–1443. https://doi.org/10.1016/j.celrep.2017.04.068.